

Filter frequency selection for manual wheelchair biomechanics

Rory A. Cooper, PhD; Carmen P. DiGiovine, PhD; Michael L. Boninger, MD; Sean D. Shimada, PhD;
Alicia M. Koontz, PhD; Mark A. Baldwin, MS

Human Engineering Research Laboratories; Departments of Rehabilitation Science and Technology and of Bioengineering, University of Pittsburgh; Department of Physical Medicine and Rehabilitation, University of Pittsburgh Medical Center; VA Pittsburgh Healthcare System, Pittsburgh, PA

Abstract—Wheelchair locomotion is an important form of mobility for many individuals with spinal cord injury. However, manual wheelchair propulsion can lead to upper-limb pain and can be very inefficient. This has led investigators to apply biomechanics to the study of wheelchair use. The objectives of this study were (1) to determine the frequency content of the motion of both hands during two speeds of wheelchair propulsion, (2) to obtain the filter frequencies necessary to remove noise from wheelchair motion data, and (3) to provide signal-to-noise ratio data for wheelchair kinematics. The participants in this study were a random sample of manual wheelchair users with paraplegia caused by spinal cord injury. Subjects propelled their personal wheelchairs on a computer-controlled dynamometer at speeds of 0.9 m/s and 1.8 m/s. Motion data were collected at 60 Hz with the use of a commercial infrared marker-based system. The main outcome measures were arm motions and noise frequency spectra, filter cutoff frequencies, and signal-to-noise ratio. Our results indicate that there is no useful signal power above 6 Hz during manual wheelchair propulsion at the speeds that we analyzed. In many cases, there was no useful signal power above 4 Hz.

This material is based on work supported by the United States Department of Veterans Affairs, Rehabilitation Research and Development Service (B869-RA), and the National Institutes of Health, National Center for Medical Rehabilitation Research (PA-93-082, and PO1 HD33989-01).

Address all correspondence and requests for reprints to Rory A. Cooper, PhD, Human Engineering Research Laboratories (151-R1), VA Pittsburgh Healthcare System, 7180 Highland Drive, Pittsburgh, PA 15206; 412-365-4850, fax: 412-365-4858, email: rcooper@pitt.edu.

This would indicate that the frequency content of manual wheelchair propulsion is similar to that of human gait. The mean signal-to-noise ratio varied from a high of 91 dB to a low of 21.8 dB. The signal-to-noise ratio was greatest in the *x* direction (along the line of progression) and lowest in the *z* direction (medial-lateral). Manual wheelchair propulsion kinematic data should be low-pass filtered at approximately 6 Hz for speeds at or below 1.8 m/s. The data presented in the archival literature appear to have been filtered at an appropriate frequency.

Key words: *filtering, frequency, motion analysis, noise reduction, wheelchairs.*

INTRODUCTION

The manual wheelchair is an important form of locomotion for individuals with spinal cord injury. Understanding the biomechanics of wheelchair propulsion may result in improved mobility and fewer episodes of pain. Kinematic studies of manual wheelchair propulsion require tracking the positions of the upper limb as functions of time. Typically, data are collected in absolute coordinates defined with respect to the laboratory setting in which the experiment is conducted.

Wheelchair propulsion studies have used either film or videotape to collect motion data [1–8]. The motion data must be processed to produce time-series data for anatomical landmarks on the upper limbs. Regardless of

the measurement system or data reduction techniques applied, noise is introduced into the signal [9–11]. Calculation of velocities and accelerations requires differentiation of the position data, which have the effect of reducing the signal-to-noise ratio (SNR) [12,13]. The SNR can be increased, and therefore, appropriate filtering can reduce error in variables associated with kinematic data.

Wheelchair propulsion motion analysis is becoming increasingly more common with the number of laboratories and clinics collecting and attempting to clinically apply the data. All motion analysis data require filtering to provide data suitable for analysis and clinical interpretation. Filtering is used to reduce the errors inherent in the data collection process so that the interpretation of the data is not unduly influenced by anomalies in the data collection that could result in false conclusions and recommendations. Studies have been presented on the importance of filtering the kinematics of racing wheelchair propulsion [14] and on the filtering of the kinetic (i.e., force and moment data) for manual wheelchair propulsion [15]. Guidelines established for filtering manual wheelchair propulsion kinematic and kinetic data are parallel to the work established for other movement activities [16].

The goal of this study was to analyze the signal and noise spectrum of kinematic data collected bilaterally during manual wheelchair propulsion at two speeds and to provide guidance for the selection of an appropriate filter cutoff frequency. Knowledge of the signal and noise spectrum can be used to select an appropriate digital filter. The purpose of this study was to determine if there were side-to-side differences in the frequency content of the motion and to determine the maximum frequency content of the third metacarpal phalangeal joint at two speeds (i.e., does the maximum frequency content change sufficiently to warrant a change in the filtering).

METHODS

Subjects

The subjects consisted of 28 individuals with paraplegia caused by a spinal cord injury. All were experienced in manual wheelchair use. The subjects included 8 women and 20 men. Only people with spinal cord injuries below T-4 were included in the study. Each subject gave written informed consent before participating, and each subject completed a medical history questionnaire.

The average age of the subjects was 36.2 ± 9.5 years, ranging from 21 to 66 years of age. The subjects had been using a wheelchair for an average of 12.9 ± 5.9 years. The mean body mass for the subjects was 76.4 ± 17.4 kg. Each subject propelled his or her personal wheelchair during testing.

Protocol

The analysis of manual wheelchair propulsion kinematic data in the frequency domain, rather than in the time domain, allowed for the determination of key signal components used in the selection of appropriate digital filters. Each subject used his or her own manual wheelchair. The only adjustment to the individual's wheelchair was the replacement of rear tires with SMART^{Wheels} [8]. The wheel position, wheel alignment, and wheel camber were the same as those for the subject's standard wheelchair wheels. The SMART^{Wheels} were used to measure the force imparted by the user onto the pushrims. The purpose of the SMART^{Wheels} for this study was to provide another means of determining the position of a marker placed on the wheel at each instant in time with the use of the optical encoder built into the SMART^{Wheels}. The wheelchair with each subject was aligned and secured over the rollers of a computer numerically controlled (CNC) dynamometer [17]. We set the resistance of the dynamometer similar to rolling over a smooth tile floor [18]. We then asked subjects to propel their wheelchair on the dynamometer for 5 minutes to become accommodated to the experimental setup. After the accommodation period, two trials were performed, one where the subject was asked to propel at 0.9 m/s, 15 W, and the other at 1.8 m/s, 30 W. Data were collected for 20 seconds after the person had maintained the desired speed for at least 10 seconds. To collect data from 56 trials from 28 subjects, we used an OPTOTRAK [19] Motion Analysis System to collect three-dimensional (3D) data of markers on the right and left third metacarpal phalangeal joint (3MP), olecranon, lateral epicondyle, ulnar styloid, radial styloid, and acromion process, as well as markers on both wheels. Data were analyzed during both the propulsion and recovery phases of the wheelchair stroke (i.e., for the complete cycle). While data were collected at multiple anatomical sites, preliminary analysis showed that the frequency content, in all directions, of the 3MP was consistently higher than the other locations. Therefore, only the data from the 3MP were selected for analysis in this study.

Data Collection

A six-camera motion analysis system, OPTOTRAK [19], is an active marker system, which allowed for the digitization of light-emitting diode (LED) markers in 3D. This system works in real time, which was calibrated prior to use with a rigid body aligned with the vertical, horizontal, and transverse axes of the laboratory. Two sets of recording devices, each consisting of three cameras, were used, one set positioned on the left side of the subject and the other set positioned on the right side of the subject, providing a bilateral view. We collected bilateral data. Because it has been shown that some manual wheelchair users exhibit asymmetries in their propulsion technique, it is possible that these asymmetries could affect the frequency content of their stroke from side to side [20]. Data were collected at 60 Hz with a shutter speed of 3,000 Hz. A pulse that the OPTOTRAK system generated was used to ensure that the OPTOTRAK and SMART^{Wheels} data collection were synchronized. We placed four LEDs (approximate size of marker was 10 mm; approximate size of light source was 1 mm) on the left and right 3MP and on the left and right SMART^{Wheels}, respectively. The LED markers on the SMART^{Wheels} were positioned 68.3 mm and 65.1 mm from the center of the hub for the left and right sides, respectively. The raw data (position of the marker) were not filtered. The position of each of the markers in 3D space was calculated in meters for each 1/60 second.

Definition of Signal and Noise

The absolute origin of the system in the laboratory coordinate system was midway between the two dynamometer drums at the level of the dynamometer cover. The positive z -axis was defined as a line that runs along the shaft of the right drum (right, left, front, and back were defined from the perspective of an individual sitting in a wheelchair that is attached to the dynamometer), while the positive y -axis was perpendicular to the plane formed by the dynamometer cover. The positive x -axis was perpendicular to the z - and y -axes. We defined the experiment coordinates by a right-hand Cartesian coordinate system. The placement and orientation of the laboratory coordinate system are depicted in **Figure 1**.

The calculation of the noise was based on the position of the hub marker given by an optical encoder integrated into the SMART^{Wheels} and the motion analysis system. First, we calculated the error between the posi-

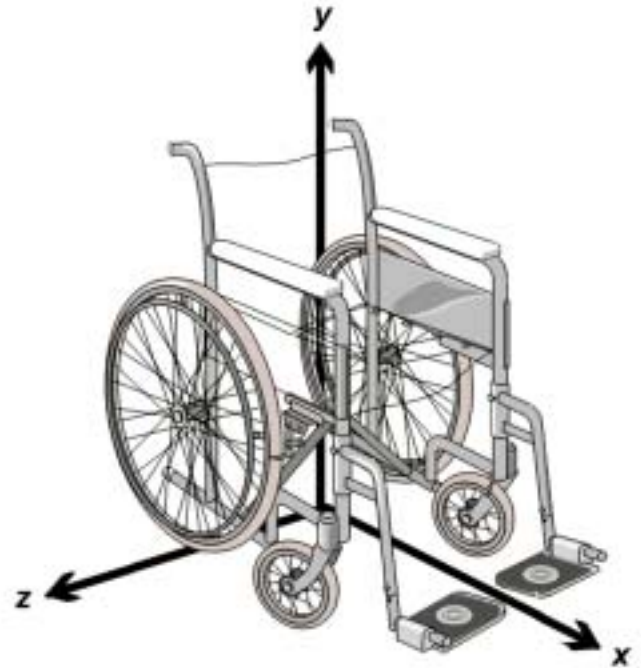


Figure 1. Cartesian coordinate system used to represent laboratory coordinate system, x , y , and z .

tion of the hub marker based on the SMART^{Wheels} data and the position of the hub marker based on the OPTOTRAK data to represent the noise in the entire system (e.g., vibration, digitizing error, optical error). This method assumes that the error from the optical encoder mounted to the wheel is negligible in comparison to the error accumulated through the data collection process of the motion analysis system. Then we subtracted the mean of the error (noise) from the difference in the x , y , and z directions, respectively. The parameter chosen to represent the signal was the 3MP minus the mean of the 3MP in the x , y , and z directions. The mean was subtracted from the signal and noise data, respectively, to remove any constant offset components. Further, the signal was referenced (i.e., the coordinates of the wheel hub were subtracted from the coordinates of the 3MP) to the wheel hub to allow comparisons across subjects with different size wheelchairs and to have a comparable reference for the two rear wheels of the wheelchair. This is equivalent to setting the origin of the motion analysis system at the center of the wheel, essentially removing the offset (i.e., zero frequency component) of the signal because of the arbitrary origin location. We attached the 3MP markers

to the skin following published methods [21,16]. The location of the 3MP, and the other anatomical markers, was found by palpation; a detailed description of the markers can be obtained in the OPTOTRAK owner's manual [19].

Frequency Analysis Methods

Using MATLAB, we performed a frequency analysis on the signal and the noise obtained from the kinematic data [22]. The analysis consisted of first applying a tapered sinusoidal window to the discrete displacement data. The tapered sinusoidal window is

$$h(kT) = \begin{cases} \sin\left[\frac{\pi}{2} \cdot \frac{kT}{0.1\tau}\right] & 0 \leq kT < 0.1\tau \\ 1 & 0.1\tau \leq kT \leq 0.9\tau \\ \cos\left[\frac{\pi}{2} \cdot \frac{kT - 0.9\tau}{0.1\tau}\right] & 0.9\tau < kT \leq \tau \end{cases} \quad (1)$$

where $h(kT)$ is the k th sample of the tapered sinusoidal window, T is the sampling interval in the time domain (1/60 s), and τ is the length of the window (20 s). We then multiplied the sampled displacement data $x(kT)$ by the tapered sinusoidal window $h(kT)$ to obtain the windowed data $y(kT)$:

$$y(kT) = x(kT) \cdot h(kT) . \quad (2)$$

Next, we used **Equation 3** to obtain the discrete Fourier transform of the windowed data

$$F(jr\Delta\omega) = \frac{\tau}{N} \sum_{k=0}^{N-1} y(kT) e^{-jr(2\pi/N)k} . \quad (3)$$

$F(jr\Delta\omega)$ is the r th sample of the Fourier transform, $\Delta\omega$ is the sampling interval in the frequency domain (0.05 Hz), and N is the total number of samples in a trial (1,200 samples). Finally, the periodogram $S(jr\Delta\omega)$ was calculated from the discrete Fourier transform using **Equation 4**. The periodogram was used to determine the cutoff frequency:

$$S(jr\Delta\omega) = \frac{1}{N} |F(jr\Delta\omega)|^2 . \quad (4)$$

In the calculation of the periodogram ($S(jr\Delta\omega)$) for each trial, the sampling frequency ($f_s = 1/T$) was 60 Hz, while the number of discrete frequency intervals (N) used in the periodogram, between 0 and 60 Hz, was equal to the number of frames in each trial (N). The analysis of the fre-

quency content only consisted of the frequencies from 0 to 30 Hz, because 30 Hz is the Nyquist frequency and the periodogram from 30 to 60 Hz is the mirror image of the periodogram from 0 Hz to 30 Hz. Therefore, no new information is obtained from the periodogram from 30 to 60 Hz.

The tapered sinusoidal window was selected because of the minimal distortion of the displacement data, while smoothly forcing the beginning 10 percent and final 10 percent of the data to zero. Also, the tapered sinusoidal window reduces the leakage of the periodogram from one frequency to another, which occurs because the displacement data are of finite length. Other windows, such as Hanning and Hamming windows [9], were examined for use in this application; however, it was determined that they significantly distorted the majority of the data in the time domain when applied across the entire trial. The size of the window was chosen to be the length of the trial because the tapered sinusoidal window was specifically chosen to be applied to the displacement data across multiple strokes rather than a single stroke. Once we calculated the periodogram, we determined the minimum frequency (which contained at least 50, 75, 90, 95, and 99 percent of the overall power, respectively, for a single trial) in each coordinate direction (x , y , and z). We present all the percentage power levels to allow the interested readers to draw their own conclusions based upon the data and their application.

RESULTS

The periodogram was created for each of the motion signals in x , y , and z (see **Figure 2**). Then we determined the mean and standard deviations of the ideal filter cutoff frequencies for each speed and overall speed in each coordinate direction (x , y , and z) (see **Tables 1–3**). We did this based on the percentage of the power (i.e., 50, 75, 90, 95, and 99 percent) across all subjects for both hands. The periodogram of each trial was then transformed into decibels (dB):

$$\text{Decibel} = 20 \cdot \log_{10} S(jr\Delta\omega) . \quad (5)$$

The periodograms for the motion signals in x , y , and z in decibels are presented in **Figure 3**. The minimum frequency for each speed and across all trials were determined when the periodogram, in decibels, dropped below a specified cutoff magnitude and stayed below that magnitude for all increasing frequencies (see **Table 4**).

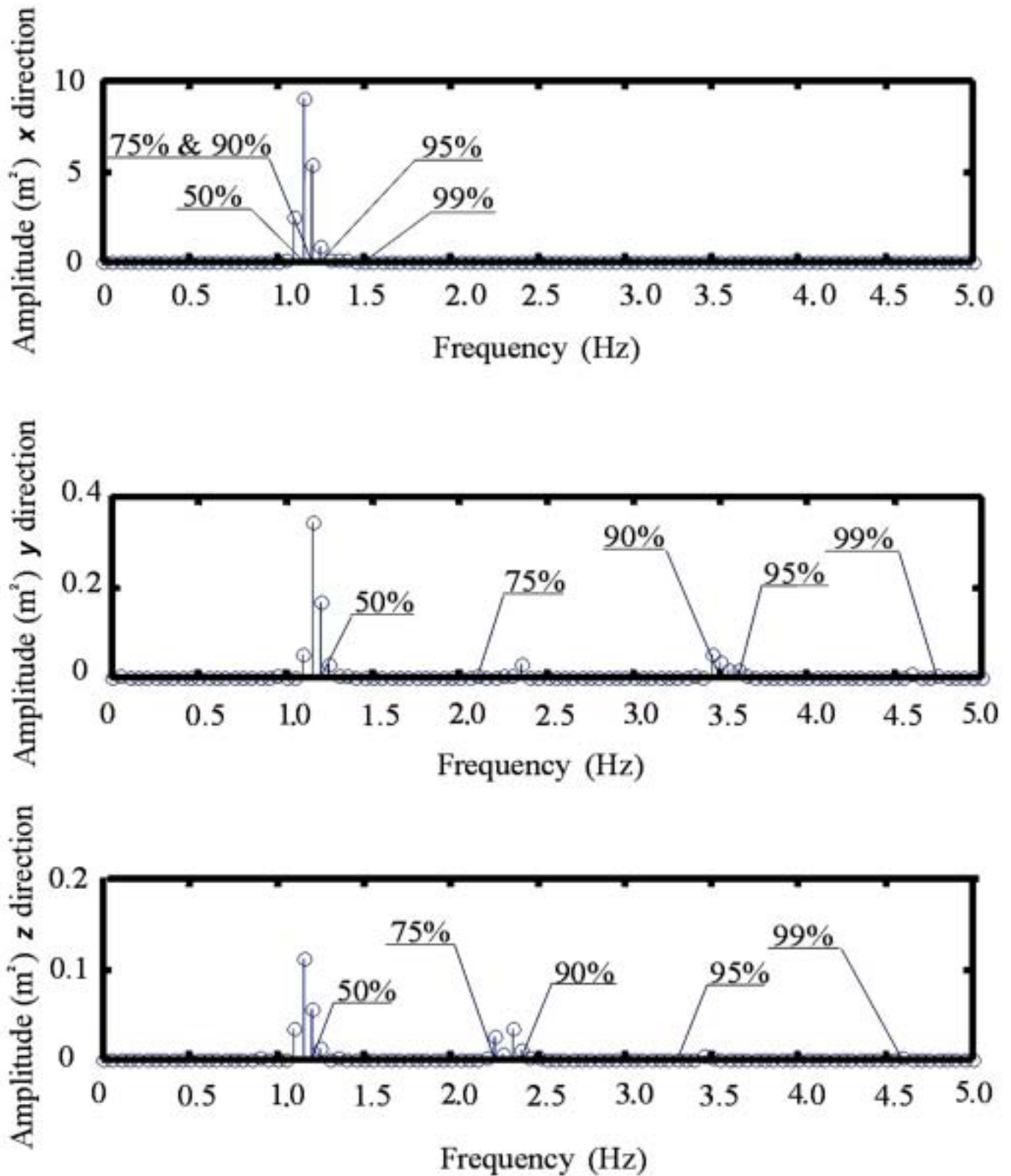


Figure 2.

Periodogram of a left side signal for a 1.8 m/s trial in x, y, and z directions, respectively. Cutoff frequency that contains 50, 75, 90, 95, and 99 percent of power is labeled for each coordinate direction.

Table 1.Cutoff frequencies based on percentage of periodogram magnitude for signal in *x* direction (*n* = 28).

Speed (m/s)	Side	Cutoff Frequency (Hz)				
		50%	75%	90%	95%	99%
0.9	Left	0.93 ± 0.15	0.94 ± 0.15	0.97 ± 0.15	1.05 ± 0.15	2.08 ± 1.18
0.9	Right	0.93 ± 0.15	0.94 ± 0.15	1.03 ± 0.37	1.22 ± 0.97	2.46 ± 3.33
1.8	Left	1.30 ± 0.25	1.32 ± 0.25	1.35 ± 0.25	1.39 ± 0.26	2.34 ± 1.01
1.8	Right	1.30 ± 0.25	1.36 ± 0.31	1.51 ± 0.86	1.71 ± 1.68	3.06 ± 4.11
All	Left	1.11 ± 0.27	1.13 ± 0.28	1.16 ± 0.28	1.22 ± 0.27	2.21 ± 1.10
All	Right	1.11 ± 0.27	1.15 ± 0.32	1.27 ± 0.70	1.46 ± 1.38	2.76 ± 3.72

Table 2.Cutoff frequencies based on percentage of periodogram magnitude for signal in *y* direction (*n* = 28).

Speed (m/s)	Side	Cutoff Frequency (Hz)				
		50%	75%	90%	95%	99%
0.9	Left	1.01 ± 0.24	1.31 ± 0.44	1.62 ± 0.52	2.21 ± 0.43	3.23 ± 0.97
0.9	Right	1.10 ± 0.32	1.23 ± 0.37	1.74 ± 0.60	2.12 ± 0.40	2.98 ± 0.49
1.8	Left	1.35 ± 0.26	1.88 ± 0.59	2.41 ± 0.82	3.02 ± 1.06	4.48 ± 2.30
1.8	Right	1.47 ± 0.40	1.76 ± 0.51	2.44 ± 0.65	2.86 ± 0.59	4.14 ± 0.63
All	Left	1.18 ± 0.30	1.60 ± 0.59	2.01 ± 0.79	2.61 ± 0.90	3.86 ± 1.86
All	Right	1.29 ± 0.40	1.49 ± 0.52	2.09 ± 0.71	2.49 ± 0.62	3.56 ± 0.81

Table 3.Cutoff frequencies based on percentage of periodogram magnitude for signal in *z* direction (*n* = 28).

Speed (m/s)	Side	Cutoff Frequency (Hz)				
		50%	75%	90%	95%	99%
0.9	Left	1.00 ± 0.31	1.40 ± 0.59	2.01 ± 1.20	2.58 ± 1.60	4.27 ± 3.36
0.9	Right	1.03 ± 0.40	1.43 ± 0.72	1.98 ± 0.75	2.50 ± 1.15	4.01 ± 3.36
1.8	Left	1.38 ± 0.51	1.79 ± 0.70	2.71 ± 1.05	3.35 ± 1.27	5.78 ± 4.03
1.8	Right	1.41 ± 0.55	1.89 ± 0.83	2.63 ± 0.94	3.28 ± 1.18	5.33 ± 3.06
All	Left	1.19 ± 0.46	1.60 ± 0.68	2.36 ± 1.17	2.97 ± 1.48	5.03 ± 3.75
All	Right	1.22 ± 0.51	1.66 ± 0.81	2.31 ± 0.90	2.89 ± 1.22	4.67 ± 3.25

The cutoff magnitudes that we used were -41, -48, and -53 dB in the *x*, *y*, and *z* directions, respectively for the left side, and -41, -55, and -56 dB in the *x*, *y*, and *z* directions, respectively, for the right side. The value of the cutoff magnitudes was chosen based on the mean plus two standard deviations of the noise periodogram.

Ensemble Average of Periodogram

We performed an ensemble average of the periodogram on each speed grouping to provide a composite of the power at each frequency across multiple subjects (see **Figure 4**). For the ensemble average of the periodogram to be calculated, the frequency intervals ($\Delta\omega$) in

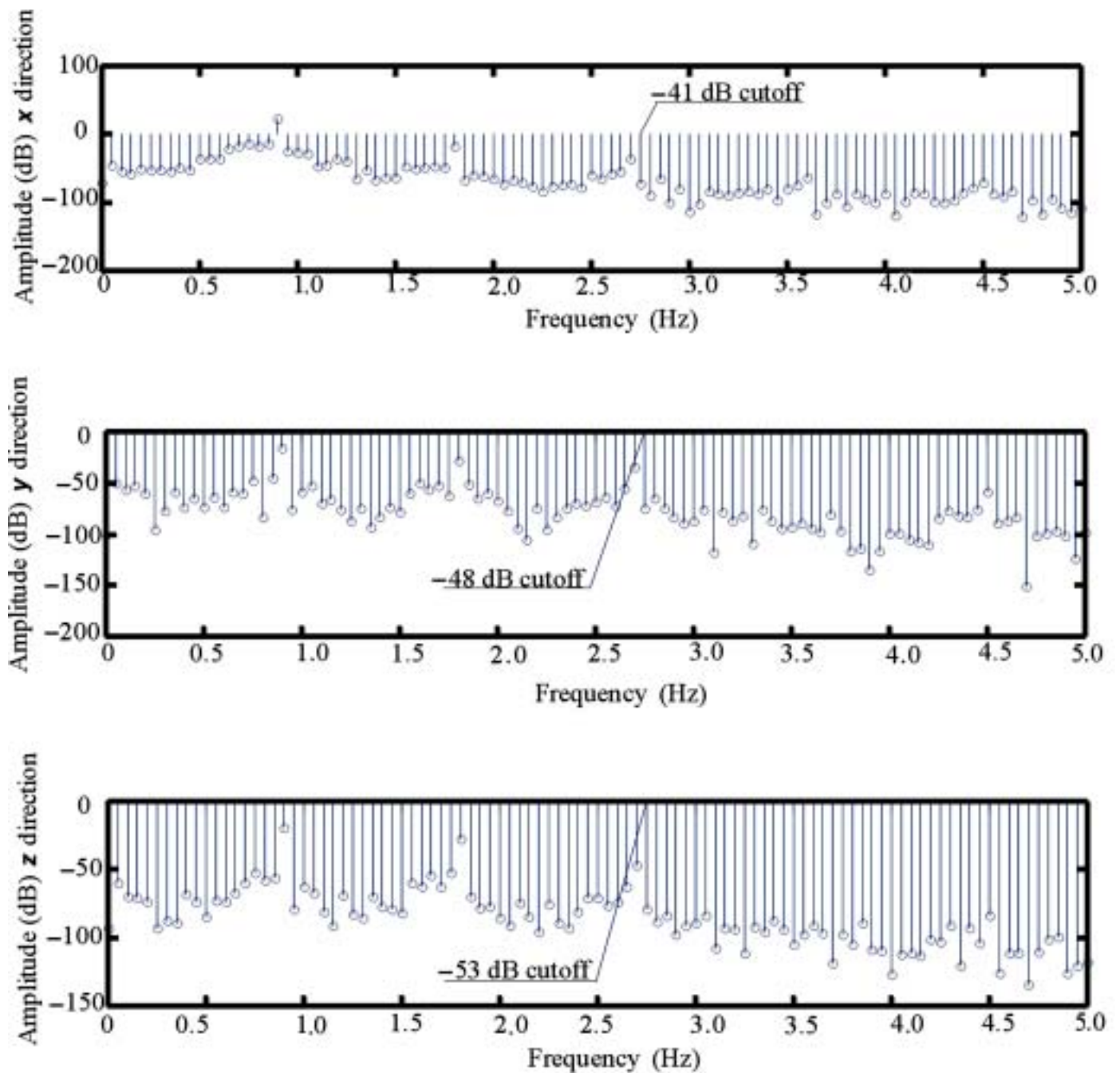


Figure 3.

Periodogram of a left signal, in decibels, for a 1.8 m/s trial in x , y , and z directions, respectively. Cutoff frequency based on mean plus two standard deviations of maximum magnitude of noise periodograms is labeled for each coordinate direction.

the periodogram had to be constant across all trials. Since each trial consisted of collecting 20 seconds (τ) of data with a sampling frequency of 60 Hz ($1/T$), the number of samples in each trial (k) and therefore in each periodogram (r) is a constant at 1,200 samples. Therefore,

neither the signal nor the noise had to be truncated or zero-padded to perform the ensemble average. Following the calculation of the ensemble average for each speed grouping and for all the trials, the minimum frequency, which contained at least 50, 75, 90, 95, and 99 percent of

Table 4.

Cutoff frequency in x , y , and z directions, respectively, when periodogram in dB for a speed grouping falls below cutoff threshold and stays below cutoff threshold. Left side cutoff thresholds are -41 , -48 , and -53 dB, in x , y , and z directions, respectively. Right side cutoff thresholds are -41 , -55 , and -56 dB in x , y , and z directions, respectively. Cutoff thresholds are based on maximum magnitude of periodogram for noise ($n = 28$).

Speed (m/s)	Side	Cutoff Frequency (Hz)		
		x	y	z
0.9	Left	2.65 ± 0.95	2.82 ± 0.55	2.43 ± 0.73
0.9	Right	2.51 ± 1.06	3.23 ± 0.61	2.64 ± 0.84
1.8	Left	3.02 ± 0.74	3.87 ± 0.64	3.34 ± 0.82
1.8	Right	3.16 ± 1.62	4.29 ± 0.69	3.37 ± 0.98
All	Left	2.83 ± 0.86	3.34 ± 0.79	2.89 ± 0.90
All	Right	2.83 ± 1.39	3.76 ± 0.84	3.00 ± 0.97

the overall power, respectively, was calculated (see **Tables 5–7**). There were differences in the cutoff frequencies for the left and right hands at 1.8 m/s, but they were not significant.

We also performed an ensemble average on the periodogram in decibels across each speed grouping and across all the trials (see **Figure 5**). Then using the cutoff magnitudes described in the previous section, the minimum frequency for each speed and overall speeds were determined when the periodogram, in decibels, dropped below and stayed below the cutoff magnitude for all higher frequencies (see **Table 8**). There were differences between the left and right side for all speeds in the y direction and at 1.8 m/s for the x and z directions.

Signal-to-Noise Ratio

We calculated the SNR based on the root mean square (rms) for an entire trial for the displacement data in each direction and for each side, respectively, using

$$\text{SNR}_{\text{rms}} = \frac{\sqrt{\frac{1}{k} \sum_{j=1}^k S_j^2}}{\sqrt{\frac{1}{k} \sum_{j=1}^k E_j^2}}, \quad (6)$$

where S is the signal, E is the noise, k is the total number of discrete points in the trial, and j is the j th point in the series. The mean and standard deviations across each speed grouping and across all the trials were calculated for both types of SNRs (see **Table 9**).

DISCUSSION

Wheelchair propulsion kinematic analysis has not benefited from the same attention to filter frequency selection as gait analysis. Winter et al. reported on one of the first studies to analyze the frequency content of motion signal and noise during human gait [10]. Their study showed that a low-pass filter with a cutoff frequency of 6 Hz was appropriate for gait analysis at normal walking speeds. They used a second-order digital Butterworth filter. When the Winter et al. paper was published, personal computers were not widely used. This may have influenced their choice of filter order. Since that time, digital signal processing has progressed dramatically.

Lesh et al. developed a computer program to implement finite impulse response (FIR) filtering for kinematic data during gait [13]. Their study showed a cutoff frequency of between 4 and 6 Hz was adequate for a low-pass FIR filter. FIR filters are simple to program, but they require large numbers of terms to achieve useful frequency roll-off above the cutoff frequency.

Antonsson and Mann studied the frequency content of gait [23]. The focus of their study was on the reduction of noise effects during differentiation. Antonsson and Mann pointed out that for low-pass filtering to be optimal, two conditions must be satisfied: (1) the noise frequencies do not overlap the signal frequencies and (2) the data must be sampled at a least twice the highest frequency of the signal and noise to avoid aliasing (i.e., the Nyquist sampling frequency).

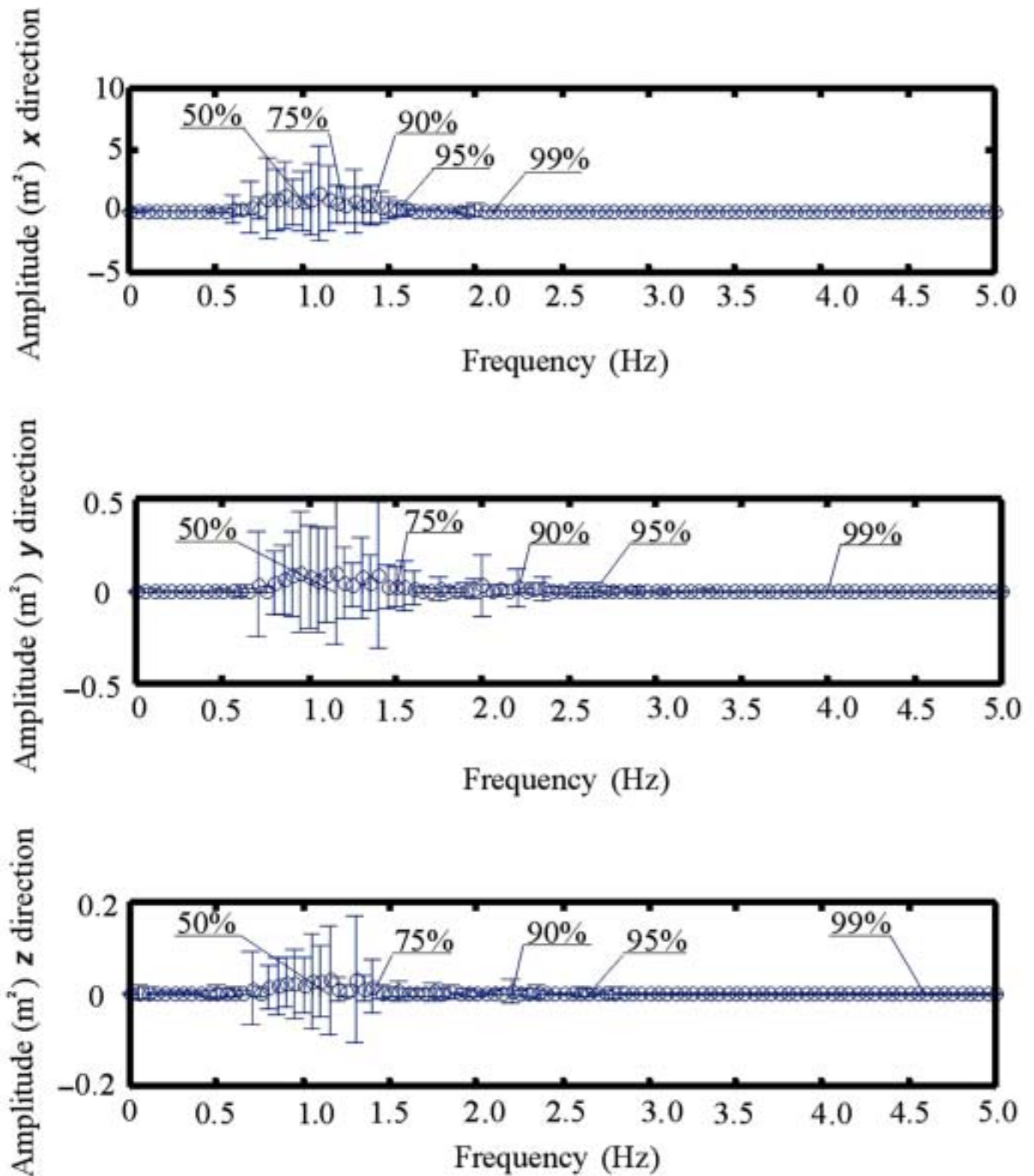


Figure 4.

Ensemble average of periodogram for all 56 trials (left side, both speeds) in x, y, and z directions, respectively. Mean and standard deviation are shown for each frequency interval. Cutoff frequency that contains 50, 75, 90, 95, and 99 percent of power is labeled for each coordinate direction.

Table 5.

Cutoff frequencies based on percentage of periodogram magnitude ensemble average for signal in *x* direction for 0.9 m/s trials, 1.8 m/s trials, and all trials combined (*n* = 28).

Speed (m/s)	Side	Cutoff Frequency (Hz)				
		50%	75%	90%	95%	99%
0.9	Left	0.90	1.00	1.15	1.25	1.95
0.9	Right	0.90	1.00	1.15	1.25	1.95
1.8	Left	1.20	1.35	1.50	1.60	2.30
1.8	Right	1.20	1.35	1.50	1.75	2.55
All	Left	1.05	1.25	1.40	1.55	2.10
All	Right	1.05	1.25	1.40	1.55	2.30

Table 6.

Cutoff frequencies based on percentage of periodogram magnitude ensemble average for signal in *y* direction for 0.9 m/s trials, 1.8 m/s trials, and all trials combined (*n* = 28).

Speed (m/s)	Side	Cutoff Frequency (Hz)				
		50%	75%	90%	95%	99%
0.9	Left	0.95	1.15	1.80	2.30	3.25
0.9	Right	0.95	1.30	1.90	2.35	3.25
1.8	Left	1.30	1.65	2.35	2.90	4.40
1.8	Right	1.35	1.95	2.40	2.90	4.10
All	Left	1.15	1.50	2.20	2.65	4.00
All	Right	1.15	1.55	2.20	2.65	3.90

Table 7.

Cutoff frequencies based on percentage of periodogram magnitude ensemble average for signal in *z* direction for 0.9 m/s trials, 1.8 m/s trials, and all trials combined (*n* = 28).

Speed (m/s)	Side	Cutoff Frequency (Hz)				
		50%	75%	90%	95%	99%
0.9	Left	0.95	1.20	1.85	2.25	3.50
0.9	Right	0.95	1.15	1.85	2.20	3.65
1.8	Left	1.30	1.45	2.45	2.90	5.60
1.8	Right	1.20	1.40	2.35	2.85	5.05
All	Left	1.15	1.40	2.20	2.65	4.60
All	Right	1.10	1.35	2.20	2.60	4.40

Angeloni et al. [24] examined the frequency content of different body segments by using the rms error method. Their study provides upper bounds for useful kinematic data for each body segment during gait. They show the optimal low-pass filter cutoff frequency to be between 5.5 and 9.8 Hz [24]. Our results indicated that there is no useful signal power above 6 Hz during manual wheelchair propulsion at the speeds that we analyzed. In many cases, there was no useful signal power above 4 Hz.

When examining the standard deviations of the ensemble average periodogram, we found that there were no notable differences in the critical frequencies. This would indicate that the frequency content of manual wheelchair propulsion is similar to that of human gait. The optimal cutoff frequency does increase moderately with speed. Therefore, higher low-pass filter frequencies may be better for speeds greater than 1.8 m/s. Our results suggest that there may be differences in the frequency content between the subjects' left and right sides. This difference likely is due to asymmetries in the propulsion stroke and instantaneous differences in wheel speeds (i.e., people tended to turn and correct small amounts even while driving straight). The left to right side differences tended to grow with increasing speed. Our results are mixed as to whether these differences are significant.

Several studies have been conducted on the kinematics of wheelchair propulsion [25–30]. However, we were unable to find any studies that dealt with issues concerning frequency analysis or filtering of data collected during manual wheelchair propulsion. The dominant trend among the reported studies of wheelchair kinematics was to refer to a study on gait or to provide no justification for the selection of filter type, filter order, or cutoff frequency. **Table 10** presents information about the filtering applied to wheelchair propulsion kinematic data from 17 studies [1,3–8,21,25,27–33]. Of the studies that provided information about filtering all used low-pass filters, most were Butterworth-type filters. The cutoff frequencies ranged from 4 to 10 Hz, and sampling frequencies ranged from 50 to 200 Hz. The filter orders ranged from second to eighth. From this review, a need is apparent for providing a foundation for appropriate filtering of wheelchair propulsion kinematic data. Our data indicate that the filter frequencies that have been reported in the literature on wheelchair propulsion are appropriate. This is encouraging because it means that the published data

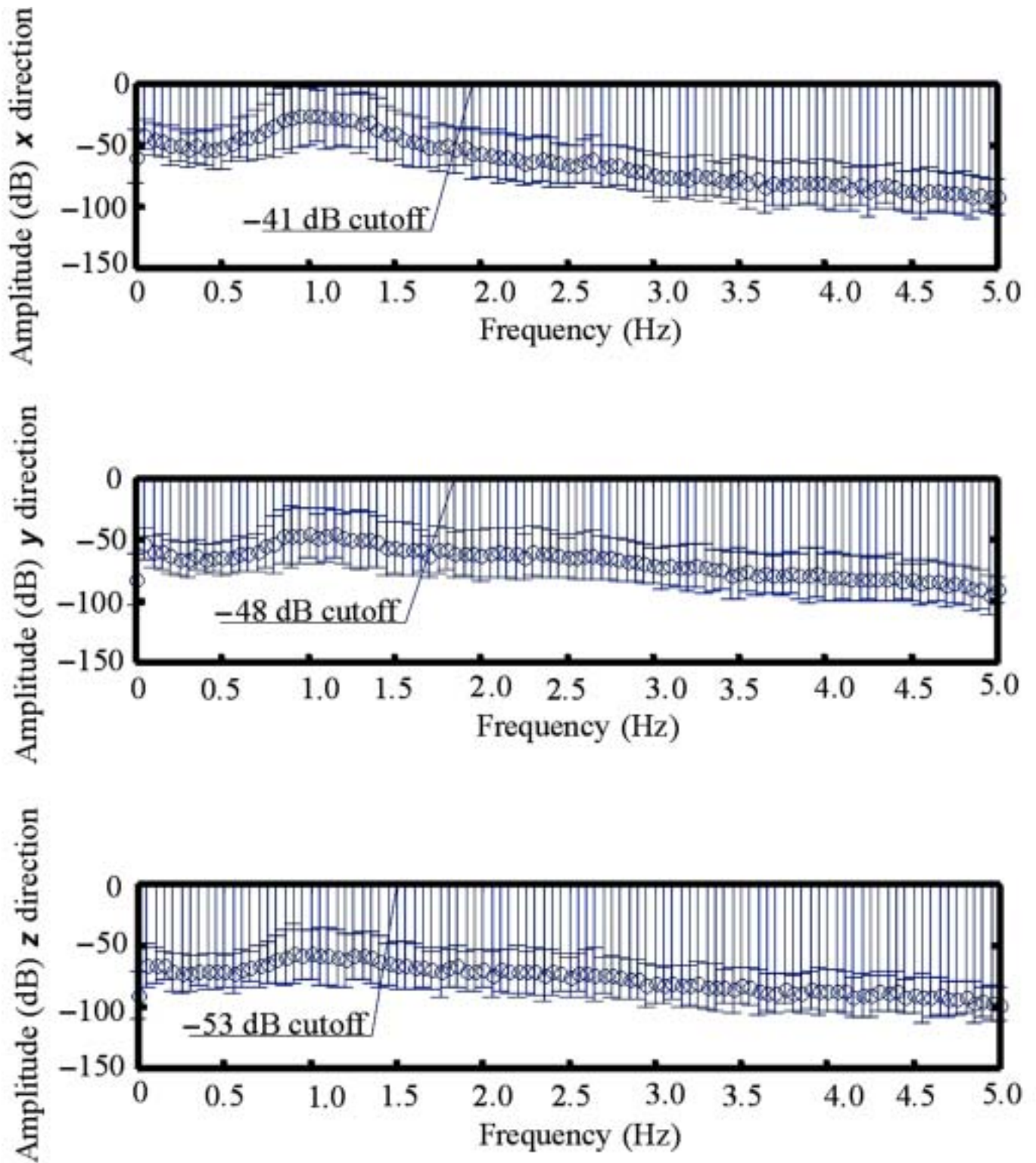


Figure 5.

Ensemble average of periodogram, in decibels, for all 56 trials (left side, both speeds) in x, y, and z directions, respectively. Mean and standard deviation are shown for each frequency interval. Cutoff frequency based on mean plus two standard deviations of maximum magnitude of noise periodograms is labeled for each coordinate direction.

Table 8.

Cutoff frequency in x , y , and z directions, respectively, when periodogram of ensemble average, in decibels, for a speed grouping falls below cutoff threshold and stays below cutoff threshold. Left side cutoff thresholds are -41 , -48 , and -53 dB, in x , y , and z directions, respectively. Right side cutoff thresholds are -41 , -55 , and -56 dB in x , y , and z directions, respectively. Cutoff thresholds are based on maximum magnitude of periodogram for noise ($n = 28$).

Speed (m/s)	Side	Cutoff Frequency (Hz)		
		x	y	z
0.9	Left	1.95	2.00	1.90
0.9	Right	2.00	2.85	1.95
1.8	Left	1.95	2.35	2.20
1.8	Right	2.20	3.35	2.40
All	Left	1.95	1.85	1.50
All	Right	1.95	2.95	1.60

have been properly filtered and should contribute to our clinical knowledge base.

This study focused on the subjects with paraplegia caused by spinal cord injury. Most likely, these subjects represent a broad class of manual wheelchair users. However, studies on individuals with tetraplegia and other neurological disorders (e.g., cerebral palsy) or orthopedic impairments should be conducted in the future as the propulsion techniques may differ from those of our subjects. As with all areas of motion analysis, the results of this study are influenced by experimental setting and protocol. The laboratory setting (e.g., lighting, temperature, and equipment) as well as the use of a dynamometer (e.g., speed, power levels) may have introduced bias into the data.

The analysis of the SNR demonstrates that when data are collected with care, noise can be controlled. The mean

SNR varied from a high of 91 dB to a low of 21.8 dB. The SNR was greatest in the x direction and lowest in the z direction. This likely is due to the coordinate system chosen. The z direction represents medial-lateral motion that constitutes the smallest range of marker motion for the reference marker. The 99-percent frequency content of the z direction is larger than the other directions because of the smaller range of motion in this direction and because of the complexity of the hand coupling (e.g., rotation about the handrim axis) [14]. The disparity in the SNR between the x and y directions may be caused by a shortcoming in the motion analysis system. The reference marker traveled a near circular path in the x - y plane. The motion analysis system that we used combines three cameras in a single housing. These cameras were aligned along a horizontal line. This can result in higher horizontal resolution than vertical resolution. However, a simple test with a calibration frame with markers of known distances placed horizontally, vertically, and medial laterally about the cameras showed that the results are acceptable in every direction and are no cause for concern.

In conclusion, our results indicate that manual wheelchair propulsion kinematic data should be low-pass filtered at approximately 6 Hz for speeds at or below 1.8 m/s. There were no significant differences ($p > 0.05$) overall in the frequency content of the signals from the left and right sides. Therefore, one can use the same filter to filter the data sets from both sides when analyzing bilateral motion data from wheelchair propulsion. However, there were some specific significant right-to-left-side differences that need to be examined in more detail in a future study. The data presented in the archival literature appear to have been filtered at an appropriate frequency.

Table 9.

Mean and standard deviations of SNR based on rms of data. Signal was defined as 3MP minus mean of 3MP, and noise was defined based on hub minus mean of hub data.

Speed (m/s)	Side	SNR of rms		
		x (Unitless (dB))	y (Unitless (dB))	z (Unitless (dB))
0.89408	Left	70.28 ± 26.34 (36.06 ± 4.50)	22.91 ± 13.36 (25.08 ± 7.08)	22.35 ± 24.06 (23.52 ± 7.60)
0.89408	Right	91.00 ± 44.23 (38.17 ± 4.36)	36.01 ± 17.27 (29.78 ± 5.55)	32.42 ± 28.69 (26.79 ± 8.25)
1.78816	Left	61.36 ± 28.99 (34.66 ± 4.79)	22.14 ± 10.74 (25.59 ± 5.40)	21.77 ± 15.79 (24.74 ± 6.10)
1.78816	Right	75.54 ± 36.91 (36.21 ± 5.53)	35.08 ± 20.45 (29.11 ± 6.21)	21.82 ± 17.15 (21.21 ± 7.12)
All	Left	65.82 ± 27.81 (35.36 ± 4.66)	22.53 ± 12.02 (25.33 ± 6.24)	22.06 ± 20.17 (24.13 ± 6.86)
All	Right	83.27 ± 41.11 (37.19 ± 5.04)	35.55 ± 18.76 (29.44 ± 5.84)	27.12 ± 24.02 (25.50 ± 7.74)

Table 10.
Sampling rate and filter parameters used in wheelchair kinematic studies.

Study	Sampling Frequency (Hz)	Filter Cutoff Frequency (Hz)	Filter Type	Filter Order
Bednarczyk & Sanderson [5], [21]	60	6	Butterworth low-pass digital filter	Fourth
Cooper et al. [8]	60	6	Butterworth zero-phase low-pass digital filter	Eighth
Mâsse et al. [30]	50	6	Butterworth low-pass	Second
Rao et al. [7]	50	4	Butterworth low-pass digital filter	Second
Rodgers et al. [1]	60	Not reported	Not reported	Not reported
Sanderson & Sommer [29]	200	4	Low-pass	Not reported
van der Linden et al. [31]	50	7	Butterworth recursive low-pass filter	Second
van der Woude et al. [32]	60	6	Butterworth recursive low-pass	Second
van der Woude et al. [33]	54	Not reported	Not reported	Not reported
Vanlandewijck et al. [4]	50	Not reported	Not reported	Not reported
Veeger et al. [28]	60	5	Butterworth filter	Second
Veeger et al. [3]	50	10	Butterworth recursive	Second
Veeger et al. [27]	50	Not reported	Not reported	Not reported
Veeger et al. [25]	90	Not reported	Not reported	Not reported
Wang et al. [6]	200	7	Butterworth low-pass digital filter	Not reported

ACKNOWLEDGMENTS

We would like to thank the subjects for their voluntary participation in this study. We would also like to thank Dr. Bob Boston for his review and comments on the manuscript.

REFERENCES

- Rodgers MM, Gayle GW, Figoni SF, Kobayashi M, Lieh J, Glaser RM. Biomechanics of wheelchair propulsion during fatigue. *Arch Phys Med Rehabil* 1994;75:85–93.
- Su FC, Lin LT, Wu HW, Chou YL, Westrich A, An KA. Three-dimensional dynamic analysis of wheelchair propulsion. *Chin J Med Biol Eng* 1993;13(4):329–42.
- Veeger HEJ, van der Woude LHV, Rozendal RH. Within-cycle characteristics of the wheelchair push in sprinting on a wheelchair ergometer. *Med Sci Sports Exerc* 1991;23(2):264–71.
- Vanlandewijck YC, Spaepen AJ, Lysens RJ. Wheelchair propulsion efficiency: movement pattern adaptations to speed changes. *Med Sci Sports Exerc* 1994;26(11):1373–81.
- Bednarczyk JH, Sanderson DJ. Kinematics of wheelchair propulsion in adults and children with spinal cord injury. *Arch Phys Med Rehabil* 1994;75:1327–34.
- Wang YT, Deutsch H, Morse M, Hedrick B, Millikan T. Three-dimensional kinematics of wheelchair propulsion across racing speeds. *Adapted Phys Activ Q* 1995;12:78–89.
- Rao SS, Bontrager EL, Gronley JK, Newsam CJ, Perry J. Three-dimensional kinematics of wheelchair propulsion. *IEEE Trans Rehabil Eng* 1996;4(3):152–60.
- Cooper RA, Robertson RN, VanSickle DP, Boninger ML, Shimada SD. Projection of the point of force application onto a planar plane of the hand during wheelchair propulsion. *IEEE Trans Rehabil Eng* 1996;4(3):133–42.
- Lathi BP. *Signals and systems*. Berkeley: Cambridge Press, Carmichael, CA. p. 194–223.
- Winter DA, Sidwall HG, Hobson DA. Measurement and reduction of noise in kinematics of locomotion. *J Biomech* 1974;7:157–59.
- Borghese NA, Ferrigno G. An algorithm for 3-D automatic movement detection by means of standard TV cameras. *IEEE Trans Biomed Eng* 1990;37(12):1221–25.
- Lanshammar H. On practical evaluation of differentiation techniques for human gait analysis. *J Biomech* 1982;15(2):99–105.
- Lesh MD, Mansour JM, Simon SR. A gait analysis subsystem for smoothing and differentiation of human motion data. *J Biomech Eng* 1979;101:205–12.
- DiGiovine CP, Cooper RA, DiGiovine MM, Boninger ML, Robertson RN. Frequency analysis of kinematics of

- racing wheelchair propulsion. *IEEE Trans Rehabil Eng* 2000;8(3):371–84.
15. Cooper RA, DiGiovine CP, Boninger CP, Shimada SD, Robertson RN. Frequency analysis of 3-dimensional pushrim forces and moments for manual wheelchair propulsion. *Automedica* 1998;16:355–65.
 16. Harris GF, Smith PA. *Human motion analysis: Current applications and future directions*. IEEE Press, New York: NY; 1996.
 17. Vosse A, Cooper RA, Dhaliwal B. Computer control of a wheelchair dynamometer. *Proceedings of the 13th Annual RESNA Conference*; 1990 June; Washington, DC. Washington: RESNA Press. p. 59–60.
 18. DiGiovine CP, Cooper RA, Dvorznak MJ. Modeling and analysis of a manual wheelchair coast down protocol. *Proceedings of the 19th Annual International Conference of the IEEE Engineering in Medicine and Biology Society*; 1997; Chicago, IL. IEEE Press. p. 1888–91.
 19. Northern Digital, Inc. *OPTOTRAK Motion Analysis System*. Ontario, Canada.
 20. Koontz AM, Cooper RA, Boninger ML. An autoregressive modeling approach to analyzing wheelchair propulsion Forces. *Med Eng Phys* 2001;23(4):285–91.
 21. Bonnier ML, Baldwin M, Cooper RA, Koontz AM, Chan L. Manual wheelchair pushrim biomechanics and axle position. *Arch Phys Med Rehabil* 2000;81(5):608–13.
 22. The Mathworks, Inc. *MATLAB reference guide*. Natick, MA; 1994.
 23. Antonsson EK, Mann RW. The frequency content of gait. *J Biomech* 1985;18(1):39–47.
 24. Angeloni C, Riley PO, DE Krebs. Frequency content of whole body gait kinematic data. *IEEE Trans Rehabil Eng* 1994;2(1):40–46.
 25. Veeger HEJ, van der Woude LHV, Rozendal RH. Effect of handrim velocity on mechanical efficiency in wheelchair propulsion. *Med Sci Sports Exerc* 1992;24(1):100–107.
 26. Bednarczyk JH, Sanderson DJ. Limitations of kinematics in the assessment of wheelchair propulsion in adults and children with spinal cord injury. *Phys Ther* 1995;75(4):281–89.
 27. Veeger HEJ, Lute EMC, Roeleveld K, van der Woude LHV. Differences in performance between trained and untrained subjects during a 30-s sprint test in a wheelchair ergometer. *Eur J App Physiol Occup Physiol* 1992;64:158–64.
 28. Veeger HEJ, van der Woude LHV, Rozendal RH. Wheelchair propulsion technique at different speeds. *Scand J Rehabil Med* 21 1989;197–203.
 29. Sanderson DJ, Sommer III. Kinematic features of wheelchair propulsion. *J Biomech* 1985;18(6):423–29.
 30. Mâsse LC, Lamontagne M, O’Riain MD. Biomechanical analysis of wheelchair propulsion for various seating positions. *J Rehabil Res Dev* 1992;29(3):12, 28.
 31. van der Linden ML, Valent L, Veeger HEJ, van der Woude LHV. The Effect of wheelchair handrim tube diameter on propulsion efficiency and force application (tube diameter and efficiency in wheelchairs). *IEEE Trans Rehabil Eng* 1996;4(2):123–32.
 32. van der Woude LHV, Veeger DJ, Rozendal RH, Sargent TJ. Seat height in handrim propulsion. *J Rehabil Res Dev* 1989;26:31–50.
 33. van der Woude LHV, Veeger HEJ, Rozendal RH. Ergonomics of wheelchair design: A prerequisite to optimum wheeling conditions. *Adap Phys Act Q* 1989;6:109–132.
- Submitted for publication July 27, 2000. Accepted in revised form January 17, 2001.